

# Newtonian and General Relativistic Models of Spherical Shells

D. Vogt\*

P. S. Letelier†

Departamento de Matemática Aplicada-IMECC, Universidade Estadual de Campinas 13083-970 Campinas, S. P., Brazil

August 27, 2018

## Abstract

A family of spherical shells with varying thickness is derived by using a simple Newtonian potential-density pair. Then, a particular isotropic form of a metric in spherical coordinates is used to construct a General Relativistic version of the Newtonian family of shells. The matter of these relativistic shells presents equal azimuthal and polar pressures, while the radial pressure is a constant times the tangential pressure. We also make a first study of stability of both the Newtonian and relativistic families of shells.

*Keywords:* gravitation.

## 1 Introduction

Distributions of matter in form of shells have been a useful tool in astrophysics and General Relativity, often providing simplified but analytically tractable models in cosmology, gravitational collapse and supernovae. In General Relativity, the pioneering work on constructing solutions of the Einstein field equations representing shells was done by Israel [1]. In his formalism, the shells are constructed by joining two manifolds across a three-dimensional time-like surface, and the matter representing the shell is interpreted as a discontinuity of the extrinsic curvature on the surface. This formalism has been used to study several models of relativistic shells.

---

\*e-mail: [dvogt@ime.unicamp.br](mailto:dvogt@ime.unicamp.br)

†e-mail: [letelier@ime.unicamp.br](mailto:letelier@ime.unicamp.br)

[2] give a brief review of some of these models and also discuss shells which admit closed equations of state, including non-linear polytropic models.

An exact solution of a static shell surrounding a black hole was obtained by [3], and the stability of such a configuration against radial perturbations was studied by [4], while non-radial perturbations were analysed by [5]. Non-radial perturbations of self-gravitating static fluid shells in the Newtonian gravity were studied by [6].

In this work, we propose a Newtonian analytical potential-density pair that represents a family of spherical shells with varying thickness. For this potential, we calculate the rotation curves of test particles and make a first study of stability of the shells by considering the stability of circular orbits of the test particles. This is done in Section 2. In Section 3, we consider a General Relativistic version of the Newtonian shells. For this task, we employ a particular isotropic form of a metric in spherical coordinates. We calculate the components of the energy-momentum tensor of the shell's matter and also analyse the geodesic circular motion of test particles and discuss their stability. Finally, in Section 4 we summarize our results.

## 2 A Model of a Newtonian Shell

In this section, we present a simple potential-density pair that describes a family of spherical shells of matter. We shall consider the following potential:

$$\Phi = -\frac{Gm}{(r^n + b^n)^{1/n}}, \quad (1)$$

where  $b > 0$  is a parameter with dimensions of length and  $n$  is a non-negative integer. By using the Poisson equation in spherical coordinates,

$$\frac{1}{r^2} \frac{d}{dr} \left( r^2 \frac{d\Phi}{dr} \right) = 4\pi G\rho, \quad (2)$$

one obtains a mass density given by

$$\rho = \frac{m(n+1)b^n r^{n-2}}{4\pi (r^n + b^n)^{2+1/n}}. \quad (3)$$

For  $n = 2$ , the pair (1) and (3) is reduced to the Plummer model [7, 8] that has a monotone decreasing density profile. However, for  $n > 2$  the density vanishes on  $r = 0$  and thus we have a shell-like distribution of matter. Fig. 1(a) shows some curves of the dimensionless mass density  $\bar{\rho} = \rho/(m/b^3)$  as

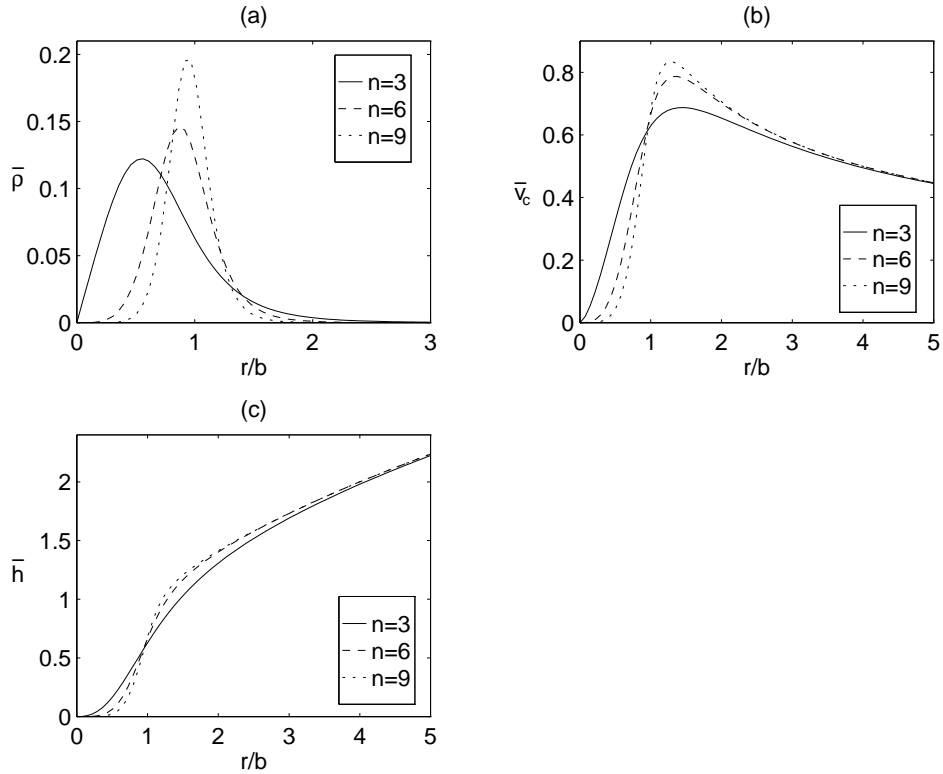


Figure 1: (a) The mass density  $\bar{\rho} = \rho/(m/b^3)$  (equation 3), as function of  $r/b$  for  $n = 3$ ,  $n = 6$  and  $n = 9$ . (b) The circular velocity  $\bar{v}_c = v_c/(Gm/b)^{1/2}$  (equation 5), and (c) the angular momentum  $\bar{h} = h/(Gmb)^{1/2}$  (equation 6) as functions of  $r/b$  for  $n = 3$ ,  $n = 6$  and  $n = 9$ .

function of  $r/b$  for  $n = 3$ ,  $n = 6$  and  $n = 9$ . For higher values of  $n$ , the mass density becomes more concentrated (thinner shell), with maximum at

$$r_{max} = \left( \frac{n-2}{n+3} \right)^{1/n} b. \quad (4)$$

For large values of  $r$ , the density (1) decays as  $1/r^{n+3}$ , thus very fast for large  $n$ , as can be seen in Fig. 1(a).

The circular velocity  $v_c = (r\Phi_{,r})^{1/2}$  and angular momentum per unit

mass  $h = rv_c$  of test particles moving in circular orbits are given by

$$v_c = \sqrt{\frac{Gmr^n}{(r^n + b^n)^{1+1/n}}}, \quad (5)$$

$$h = \sqrt{\frac{Gmr^{n+2}}{(r^n + b^n)^{1+1/n}}}. \quad (6)$$

Curves of the circular velocity  $\bar{v}_c = v_c/(Gm/b)^{1/2}$  and of the angular momentum  $\bar{h} = h/(Gmb)^{1/2}$  for  $n = 3$ ,  $n = 6$  and  $n = 9$  are depicted in Figs 1(b) and (c), respectively. The stability of circular orbits can be determined using the Rayleigh criterion of stability for a rotating fluid ([9]; see also [10]), and that can be adapted to study circular orbits of test particles in self-gravitating systems (see e. g. [11] for an application of the Rayleigh criterion of stability in General Relativity). The condition for a stable orbit is

$$h \frac{dh}{dr} > 0. \quad (7)$$

Using equation (6), it is straightforward to check that the orbits are always stable.

It is instructive to consider the limit  $n \rightarrow \infty$ . In this case, we have an infinitesimal thin shell on  $r = b$ , and the limits of the potential (1) and circular velocity (5) are

$$\Phi = \begin{cases} -\frac{Gm}{b} & \text{if } 0 \leq r < b, \\ -\frac{Gm}{r} & \text{if } r \geq b, \end{cases} \quad (8)$$

$$v_c = \begin{cases} 0 & \text{if } 0 \leq r < b, \\ \sqrt{\frac{Gm}{r}} & \text{if } r \geq b. \end{cases} \quad (9)$$

Thus, for  $r < b$  the potential is constant and a test particle is at rest inside the shell, and if  $r \geq b$  the shell exerts on the test particle the same gravitational force as a point mass located on  $r = 0$ , in agreement with Newton's Shell Theorem.

### 3 A Model of a General Relativistic Shell

Now, we study a General Relativistic version of the Newtonian potential-density pair discussed in the previous section. For this, it is convenient

to choose a particular metric in isotropic form in spherical coordinates  $(t, r, \theta, \varphi)$ , which we write as

$$ds^2 = \left( \frac{1-f}{1+f} \right)^2 c^2 dt^2 - (1+f)^4 (dr^2 + r^2 d\theta^2 + r^2 \sin^2 \theta d\varphi^2), \quad (10)$$

where  $f = f(r)$ . In this particular form of metric, the Schwarzschild solution is given by  $f = Gm/(2c^2 r)$ . A similar form of the metric (10) in cylindrical coordinates was used by [12] to construct General Relativistic versions of Newtonian models for distributions of matter in galaxies.

For metric (10), the Einstein equations  $G_{\mu\nu} = -(8\pi G/c^4)T_{\mu\nu}$  yield the following expressions for the non-zero components of the energy-momentum tensor  $T_{\mu\nu}$ :

$$T_t^t = -\frac{c^4}{2\pi G (1+f)^5} \frac{1}{r^2} \frac{d}{dr} \left( r^2 \frac{df}{dr} \right), \quad (11)$$

$$T_r^r = \frac{c^4}{2\pi G (1+f)^5 (1-f)} \frac{df}{dr} \left( \frac{f}{r} + \frac{df}{dr} \right), \quad (12)$$

$$T_\theta^\theta = T_\varphi^\varphi = \frac{c^4}{4\pi G (1+f)^5 (1-f)} \left[ f \frac{d^2 f}{dr^2} + \frac{f}{r} \frac{df}{dr} - \left( \frac{df}{dr} \right)^2 \right]. \quad (13)$$

Because  $T_{\mu\nu}$  has only diagonal non-zero components, the energy density is directly given by  $\epsilon = T_t^t/c^2$  and the pressures or tensions along a direction  $k$  read  $P_k = -T_k^k$ . The ‘effective Newtonian density’  $\rho_N = \epsilon + P_r/c^2 + P_\theta/c^2 + P_\varphi/c^2$  reads

$$\rho_N = -\frac{c^2}{2\pi G (1+f)^5 (1-f)} \frac{1}{r^2} \frac{d}{dr} \left( r^2 \frac{df}{dr} \right). \quad (14)$$

The relation between the function  $f(r)$  and the Newtonian potential  $\Phi(r)$  is obtained by comparing equation (14) or (11) with equation (2) in the non-relativistic limit when  $f \ll 1$ ,

$$f = -\frac{\Phi}{2c^2}. \quad (15)$$

Now, using equation (15) with the potential (1), equations (11)–(14) can

be cast as

$$\bar{\epsilon} = \frac{(n+1)\bar{b}^n\bar{r}^{n-2}}{4\pi\xi^{2-4/n}(1+\xi^{1/n})^5}, \quad (16)$$

$$\bar{P}_r = \frac{\bar{b}^n\bar{r}^{n-2}}{4\pi\xi^{2-4/n}(-1+\xi^{1/n})(1+\xi^{1/n})^5}, \quad (17)$$

$$\bar{P}_\theta = \bar{P}_\varphi = \frac{n\bar{b}^n\bar{r}^{n-2}}{8\pi\xi^{2-4/n}(-1+\xi^{1/n})(1+\xi^{1/n})^5}, \quad (18)$$

$$\bar{\rho}_N = \frac{(n+1)\bar{b}^n\bar{r}^{n-2}}{4\pi\xi^{2-5/n}(-1+\xi^{1/n})(1+\xi^{1/n})^5}, \quad (19)$$

where the dimensionless variables and parameters are as follows:  $\bar{r} = r/r_s$ ,  $\bar{b} = b/r_s$ ,  $\bar{\epsilon} = \epsilon/(m/r_s^3)$ ,  $\bar{\rho}_N = \rho_N/(m/r_s^3)$ ,  $\bar{P}_k = P_k/(mc^2/r_s^3)$ , and where we defined  $r_s = Gm/(2c^2)$  and  $\xi = \bar{r}^n + \bar{b}^n$ . We assume again that  $n > 2$ . For  $n = 2$ , equations (16)–(19) reduce to the perfect fluid sphere derived by [13], which has as equation of state similar to the classical polytrope of index 5. Note that the relation between  $\bar{P}_r$  and  $\bar{P}_\theta$  is independent of the radius and is simply  $\bar{P}_r = 2\bar{P}_\theta/n$ .

In order to be physically meaningful, the components of the energy-momentum tensor should satisfy the energy conditions. The strong energy condition states that  $\rho_N \geq 0$ , whereas the weak energy condition imposes the condition  $\epsilon \geq 0$ . The dominant energy condition requires  $|P_k/\epsilon| \leq c^2$ . Equations (16)–(19) show that the weak energy condition is always satisfied, and the strong condition holds if  $\bar{b} \geq 1$ . This condition also ensures that we have pressures everywhere. The inequality  $|P_r/\epsilon| \leq c^2$  is satisfied when  $\bar{b} \geq (n+2)/(n+1)$ , and we have  $|P_\theta/\epsilon| \leq c^2$  if  $\bar{b} \geq (3n+2)/(2n+2)$ . Thus, there exists an interval of the parameter  $\bar{b}$  where all energy conditions are satisfied.

Figs 2(a)–(d) display, respectively, some curves of the energy density  $\bar{\epsilon}$ , the effective Newtonian density  $\bar{\rho}_N$ , the radial pressure  $\bar{P}_r$  and the azimuthal/polar pressure  $\bar{P}_\theta$  as functions of the radial coordinate for the shell with  $n = 3$  and parameter values  $\bar{b} = 2, 2.5$  and  $3$ . In Figs 3(a)–(d), the same quantities are displayed for the shell with  $n = 6$  and parameter values  $\bar{b} = 2.5, 3$  and  $3.5$ . All quantities have the profile of a shell-like distribution of matter. As the value of the parameter  $\bar{b}$  is increased, the densities and pressures are smoothed out. The densities and pressures become more concentrated when  $n$  is increased.

As we did in the Newtonian model, we also study the circular orbits and stability of test particles. Without loss of generality, if the geodesic motion

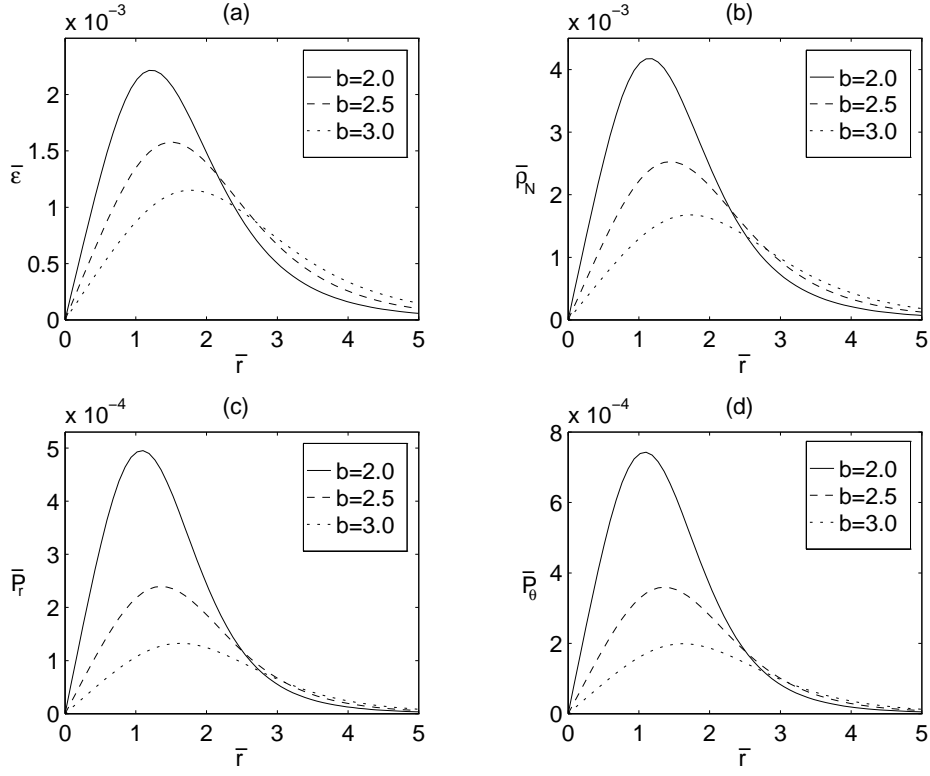


Figure 2: (a) The energy density  $\bar{\epsilon} = \epsilon/(m/r_s^3)$  (equation 16), (b) the effective Newtonian density  $\bar{\rho}_N = \rho_N/(m/r_s^3)$  (equation 19), (c) the radial pressure  $\bar{P}_r = P_r/(mc^2/r_s^3)$  (equation 17) and (d) the azimuthal/polar pressure  $\bar{P}_\theta = P_\theta/(mc^2/r_s^3)$  (equation 18) as functions of  $\bar{r} = r/r_s$  for  $n = 3$ , and parameter  $\bar{b} = b/r_s = 2, 2.5$  and  $3$ .

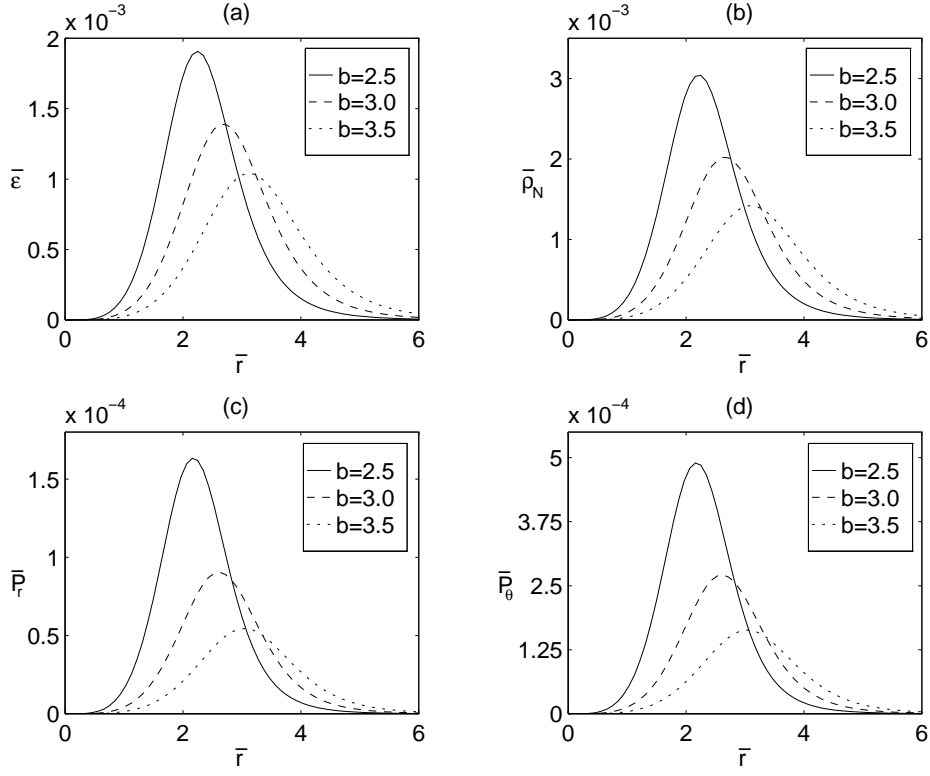


Figure 3: (a) The energy density  $\bar{\epsilon} = \epsilon/(m/r_s^3)$  (equation 16), (b) the effective Newtonian density  $\bar{\rho}_N = \rho_N/(m/r_s^3)$  (equation 19), (c) the radial pressure  $\bar{P}_r = P_r/(mc^2/r_s^3)$  (equation 17) and (d) the azimuthal/polar pressure  $\bar{P}_\theta = P_\theta/(mc^2/r_s^3)$  (equation 18) as functions of  $\bar{r} = r/r_s$  for  $n = 6$ , and parameter  $\bar{b} = b/r_s = 2.5, 3$  and  $3.5$ .



$n$	3	4	5	6	7	8	9
$\bar{b}_{min.}$	1.78	2.00	2.18	2.32	2.43	2.52	2.60

Table 1: Approximate minimum values of the parameter  $\bar{b} = b/r_s$  that ensures subluminal rotation curves for some values of  $n$ .

is confined on the  $\theta = \pi/2$  plane, the expressions for the circular velocity and for the angular momentum are formally the same as in cylindrical coordinates, and we have [12]

$$v_c = \sqrt{\frac{-2c^2 r f_{,r}}{(1-f)(1+f+2rf_{,r})}}, \quad (20)$$

$$h = cr^2 (1+f)^2 \sqrt{\frac{-2f_{,r}}{r[1-f^2+2rf_{,r}(2-f)]}}. \quad (21)$$

For the shell potential (1), we get

$$\bar{v}_c = \sqrt{\frac{2\bar{r}^n \xi^{1/n}}{(-1 + \xi^{1/n})(\bar{b}^n - \bar{r}^n + \xi^{1+1/n})}}, \quad (22)$$

$$\bar{h} = \frac{\sqrt{2}\bar{r}^{1+n/2} (1 + \xi^{1/n})^2}{\xi^{3/(2n)} \sqrt{\bar{r}^n - \bar{b}^n + \xi^{1+2/n} - 4\bar{r}^n \xi^{1/n}}}, \quad (23)$$

where  $\bar{v}_c = v_c/c$ ,  $\bar{h} = r_s c$  and  $\xi = \bar{r}^n + \bar{b}^n$ .

Some curves of the circular velocity  $\bar{v}_c = v_c/c$  and angular momentum  $\bar{h} = r_s c$  for relativistic shells are shown in Figs 4(a)–(d). In Figs 4(a)–(b), the curves of rotation are displayed for the shells with  $n = 3$  and  $n = 6$ , respectively, and the corresponding curves of angular momentum are plotted in Figs 4(c)–(d). As the values of the parameter  $\bar{b} = b/r_s$  is increased, the velocities becomes less relativistic. The minimum value of  $\bar{b}$  such that the rotation curve is subluminal has to be found numerically. Table 1 shows some approximate minimum values for  $\bar{b}$  for shells with  $n = 3$  to  $n = 9$ . Note that these minimum values are always larger than those required by the energy conditions.

The curves of angular momentum in Figs 4(c)–(d) show regions of instability at high relativistic velocities. In the Newtonian limit, the orbits are always stable, thus this instability is a purely relativistic effect. Using the Rayleigh criterion of stability, curves of  $d\bar{h}/d\bar{r} = 0$  as functions of  $\bar{r}$  and  $\bar{b}$  are shown in Fig. 5 for models of shells with  $n$  from  $n = 3$  to  $n = 6$ . In each graph, the minimum value of  $\bar{b}$  is that given in Table 1. In the inner part of

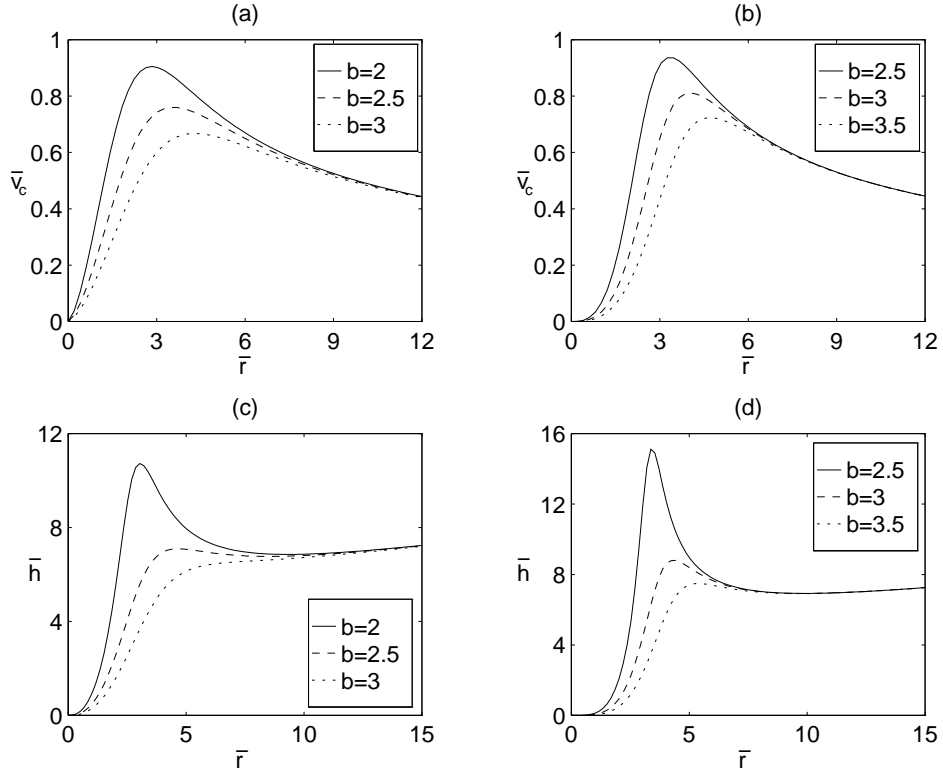


Figure 4: (a)–(b) The circular velocity  $\bar{v}_c = v_c/c$  (equation 22), as a function of  $\bar{r} = r/r_s$  for the relativistic shell model with (a)  $n = 3$  and (b)  $n = 6$ . (c)–(d) The angular momentum  $\bar{h} = r_s c$  (equation 23), as a function of  $\bar{r} = r/r_s$  for the relativistic shell model with (c)  $n = 3$  and (d)  $n = 6$ .

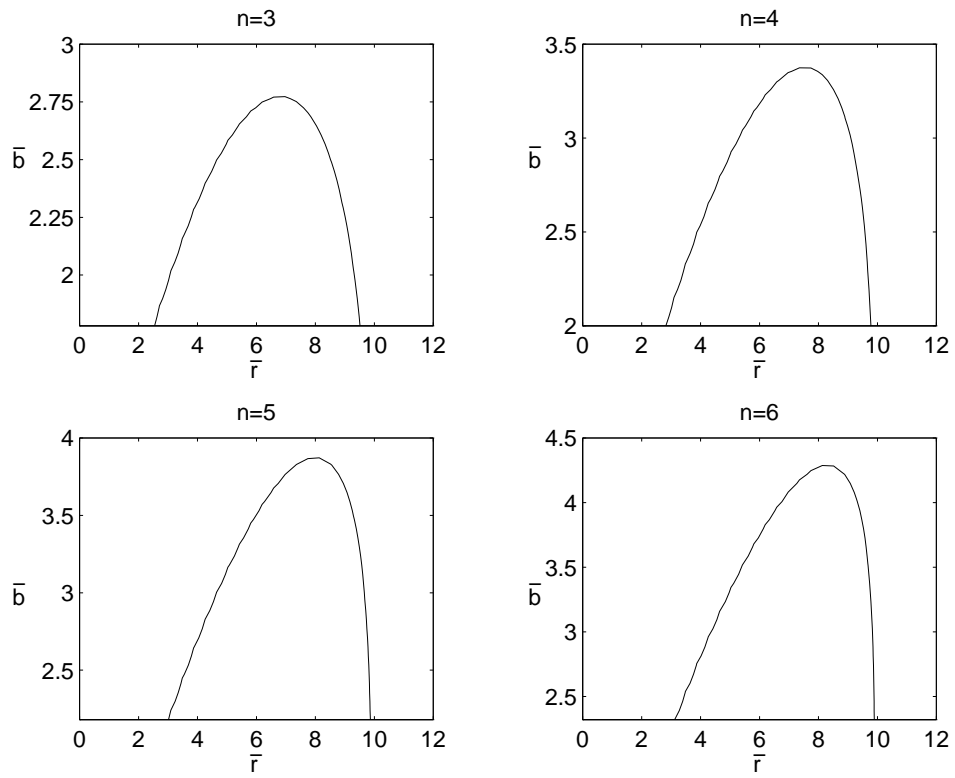


Figure 5: Curves of  $d\bar{h}/d\bar{r} = 0$  as functions of  $\bar{r}$  and  $\bar{b}$  for circular geodesic orbits in shells with  $n = 3$  to  $n = 6$ .

the curves, orbits are unstable. The regions of instability become larger as the parameter  $n$  is increased.

## 4 Discussion

We proposed a very simple potential-density pair in Newtonian gravity that describes a family of spherical shells whose thickness is function of a parameter  $n$ . In the limit  $n \rightarrow \infty$ , one obtains an infinitesimal thin shell. This family of shells is found to be stable by the Rayleigh criterion of stability. We also studied a General Relativistic version of the Newtonian model of shells by using a particular metric in isotropic form in spherical coordinates. These relativistic shells have radial pressures that are different from the equal azimuthal and polar pressures, but are proportional to for a fixed value of  $n$ . Also, parameters can be chosen such that the matter in the shells satisfies all the energy conditions. The Rayleigh criterion of stability shows that the relativistic shells have regions of unstable circular orbits of test particles, and this instability is a pure relativistic effect.

## Acknowledgments

D. V. thanks FAPESP for financial support, and P. S. L. thanks FAPESP and CNPq for financial support.

## References

- [1] Israel W., 1966, Nuovo Cimento B, 44, 1 Nuovo Cimento B, 48, 463 (erratum).
- [2] Kijowski J., Magli G., Malafarina D., 2006, Gen. Relativ. Gravitation, 38, 1697.
- [3] Frauendiener J., Hoenselaers C., Konrad W., 1990, Classical Quantum Gravity, 7, 585.
- [4] Brady P.R., Louko J., Poisson E., 1991, Phys. Rev. D, 44, 1891.
- [5] Schmidt B.G., 1998, Phys. Rev. D, 59, 024005.
- [6] Bičák J., Schmidt B.G., 1999, ApJ, 521, 708.
- [7] Plummer H.C., 1911, MNRAS, 71, 460.

- [8] Binney J., Tremaine S., 2008, *Galactic Dynamics*, 2nd edn. Princeton Univ. Press, Princeton, NJ.
- [9] Rayleigh J.W.S., 1917, *Proc. R. Soc. London A*, 93, 148.
- [10] Landau L.D., Lifshitz E.M., *Fluid Mechanics*, 2nd edn. Pergamon Press, Oxford.
- [11] Letelier P.S., 2003, *Phys. Rev. D*, 68, 104002.
- [12] Vogt D., Letelier P.S., 2005, *MNRAS*, 363, 268.
- [13] Buchdahl H.A., 1964, *ApJ*, 140, 1512.